The promyelocytic leukemia protein functions as a negative regulator of IFN-γ signaling

Youn-Hee Choi*, Rosa Bernardi†, Pier Paolo Pandolfi†, and Etty N. Benveniste*‡

*Department of Cell Biology, University of Alabama, Birmingham, AL 35294; and †Cancer Biology and Genetics Program, Department of Pathology and Medicine, Sloan–Kettering Institute, Memorial Sloan–Kettering Cancer Center, New York, NY 10021

IFN-γ is an immunomodulatory cytokine and uses the STAT-1α transcription factor to mediate gene expression. The promyelocytic leukemia (PML) protein regulates transcription as an activator or repressor, depending on the gene under investigation. Herein, we examined the influence of PML on IFN-γ signaling, using PML wild-type ($Pml^{+/+}$) and deficient ($Pml^{-/-}$) mouse embryonic fibroblasts (MEF). $Pml^{-/-}$ MEF exhibit enhanced IFN-γ-induced STAT-1α transcriptional activity compared with $Pml^{+/+}$ cells. Moreover, reconstitution of PML in $Pml^{-/-}$ MEF reduced STAT-1α transcriptional activity to levels comparable to $Pml^{+/+}$ MEF. Numerous endogenous IFN-γ-regulated genes were up-regulated in $Pml^{-/-}$ MEF compared with $Pml^{+/+}$ MEF. IFN-γ-mediated STAT-1α DNA-binding activity was enhanced in $Pml^{-/-}$ cells compared with $Pml^{+/+}$ cells. Lastly, IFN-γ enhanced the formation of a PML–STAT-1α complex in the nucleus. These data suggest a novel function for PML in the IFN-γ signaling pathway by inhibiting STAT-1α DNA binding and transcriptional activity.

signal transduction | STAT

IFN-γ is an immunomodulatory cytokine that mediates its biological responses through the JAK-STAT signaling pathway (1). Binding of IFN-γ to its receptor induces the oligomerization of the receptor subunits and activation of JAK1 and JAK2 tyrosine kinases, which are associated with IFNGR1 and IFNGR2, respectively. The phosphorylation of a tyrosine residue on IFNGR1 by activated JAKs provides a docking site for STAT-1α. Bound STAT-1α becomes phosphorylated on tyrosine 701, dissociates from the receptor complex, homodimerizes, translocates into the nucleus, and binds a DNA sequence [gamma-activated site (GAS)], leading to transcriptional activation of IFN-γ-stimulated genes (2). Serine 727 of STAT-1α is phosphorylated by other kinases such as MAPK, PI3K, and mTOR, and is critical for optimal STAT-1α transcriptional activity (3). IFN-γ activation of the JAK-STAT pathway is attenuated by negative regulators such as suppressors of cytokine signaling (SOCS), protein tyrosine phosphatases, and protein inhibitors of activated STATs (PIAS) (4). The SOCS-1 protein inhibits JAK2 kinase activity and attenuates STAT-1α phosphorylation and activation (5). Phosphatases dephosphorylate the tyrosine residues of the IFN-γ receptor, JAKs and STATs (6). PIAS1 binds to activated STAT-1α dimers in the nucleus and inhibits their DNA-binding activity (7). More recently, other proteins such as TRADD and activated vitamin D3 hormone have been shown to inhibit IFN-γ-mediated signaling (8, 9).

The promyelocytic leukemia (Pml) gene was identified through its fusion to the retinoic acid receptor-α involved in the t(15;17) chromosomal translocation associated with acute PML (10–14). The Pml gene is widely expressed and is enhanced by stimuli such as interferons, viral infection, heat shock, and γ-irradiation (15). PML is a growth/tumor suppressor protein which regulates cell cycle progression, gene transcription, and apoptosis. Various PML isoforms have been identified that share the same N terminus with variable C termini generated by alternative splicing (16). PML is localized to subnuclear structures called PML-Nuclear Bodies, which recruit critical regula-

tors of cell proliferation, apoptosis, genome stability, and post-translational modifications (17). Several studies demonstrate a role for PML in transcriptional regulation through its association with the coactivator CREB-binding protein; corepressors such as HDAC, N-CoR, and mSin3A; and transcription factors such as Nur77, AP-1, myc, and p53 (18–24). One cytoplasmic isoform of PML has recently been shown to serve as a critical regulator of the TGF-β1 signaling pathway (25).

Herein, we demonstrate a function of PML as a negative regulator of IFN-γ signaling. In a preliminary screen for STAT-1α-binding proteins, PML was found to interact with STAT-1α in an IFN-γ-dependent manner. We examined the effect of PML on the transcriptional activity of STAT-1α using $Pml^{+/+}$ and $Pml^{-/-}$ mouse embryonic fibroblasts (MEF). $Pml^{-/-}$ MEF demonstrated enhanced IFN-γ-induced STAT-1α transcriptional activity compared with $Pml^{+/+}$ MEF, which was reduced by reconstitution of PML. Correspondingly, IFN-γ-dependent endogenous gene induction was enhanced in $Pml^{-/-}$ compared with $Pml^{+/+}$ MEF. Furthermore, PML inhibited IFN-γ-mediated STAT-1α DNA-binding activity. IFN-γ enhanced the formation of a PML–STAT-1α complex, and the C terminus of PML was responsible for STAT-1 binding. Collectively, these results demonstrate a regulatory role for PML in the IFN-γ signaling pathway by inhibiting IFN-γ-induced STAT-1α transcriptional activity.

Results

PML Represses IFN-γ-Induced STAT-1α Transcriptional Activity. We initially examined the influence of PML on IFN-γ-induced STAT-1α transcriptional activity. $Pml^{+/+}$ and $Pml^{-/-}$ MEF were transiently transfected with three different luciferase reporter constructs containing GAS elements; the minimal class II transactivator (CIITA) promoter with one GAS element (CIITAp-D4), full length CIITA promoter containing three GAS elements (CIITA), and a tandem array of four GAS elements (GAS4; Fig. 1 A–C). In $Pml^{+/+}$ MEF, IFN-γ induced luciferase activity by ≈4.0-, ≈11.0-, and ≈17.0-fold for the three GAS reporter constructs, whereas in the $Pml^{-/-}$ MEF, IFN-γ treatment led to a ≈27.3-, ≈131.7-, and ≈52.2-fold increase in luciferase activity, respectively. Enhanced IFN-γ-induced STAT-1α transcriptional activity was also observed in primary $Pml^{-/-}$ MEF (≈13.6-fold) compared with primary $Pml^{+/+}$ MEF (≈7.5-fold; Fig. 1D). To determine whether PML influenced IFN-γ-induced transcriptional activity, $Pml^{-/-}$ MEF were reconstituted with three
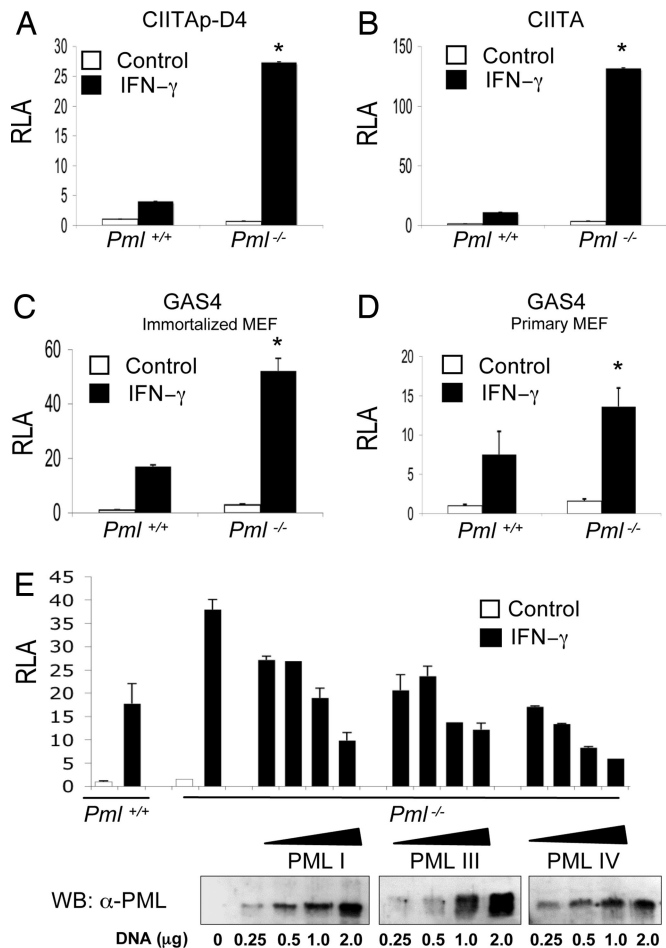
IMMUNOLOGY

Fig. 1. PML represses IFN-γ-induced STAT-1α transcriptional activity. Immortalized *Pml*^{+/+} or *Pml*^{−/−} MEF were transfected with the minimal CIITA reporter containing one GAS element (CIITAp-D4; *A*), the full length CIITA reporter containing three GAS elements (CIITA; *B*), or the GAS4 reporter that contains four GAS elements (GAS4; *C*). (*D*) Primary MEF were also tested with the GAS4 reporter. (*E*) Reintroduction of PML isoforms in *Pml*^{−/−} MEF. Immortalized *Pml*^{+/+} or *Pml*^{−/−} MEF were cotransfected with the GAS4 reporter and/or increasing concentrations of PML I, PML III, and PML IV expression vectors (0–2 μg), and equal molar concentrations of empty vector. (*Lower*) Immunoblot analysis of *Pml*^{−/−} MEF transfected with PML I, PML III, and PML IV. Cells were either untreated or treated with IFN-γ (10 ng/ml) for 16 h, and then luciferase activity was determined. Data are presented as fold increase in relative luciferase activity (RLA) compared with RLA in the absence of IFN-γ. Values are the mean ± SD of three separate experiments. *, *P* < 0.05.

different PML isoforms, PML I, PML III, and PML IV. Reconstitution of PML reduced IFN-γ-induced STAT-1α transcriptional activity in a dose-dependent manner to levels comparable to *Pml*^{+/+} MEF or to a lesser extent with higher concentrations of PML (Fig. 1*E*). Although the three PML isoforms showed varying degrees of expression (Fig. 1*E Lower*) and repression, all three suppressed IFN-γ-induced STAT-1α transcriptional activity.

PML Influences IFN-γ-Regulated Genes. The effect of PML on endogenous genes regulated by IFN-γ was examined by microarray analysis. *Pml*^{+/+} and *Pml*^{−/−} MEF cells were incubated in the absence or presence of IFN-γ for 4 h, and then mRNA was harvested and subjected to the Affymetrix (Santa Clara, CA) mouse GeneChip. Fig. 2*A* shows the proportion of affected genes (2-fold change in expression) that are either up- or down-regulated between untreated and IFN-γ-treated cells. In *Pml*^{+/+} MEF, IFN-γ
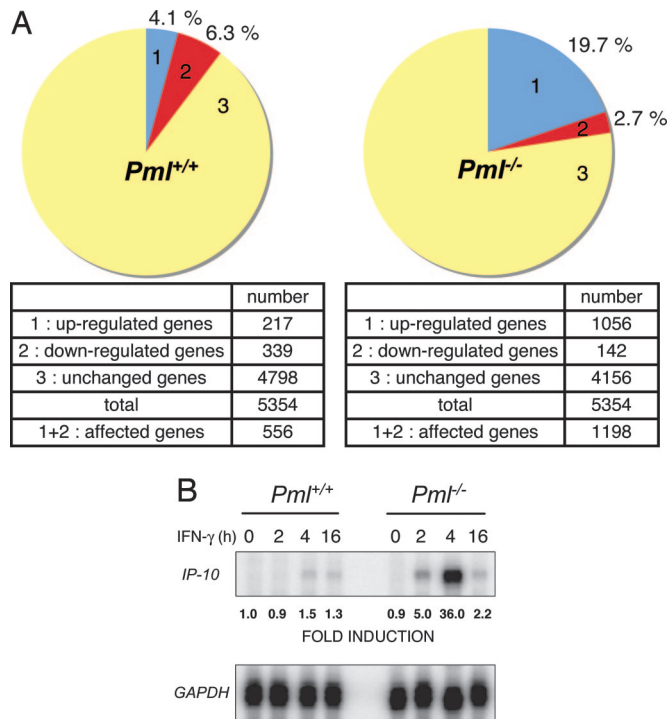

Fig. 2. PML influences IFN-γ-regulated genes. (*A*) RNA from immortalized *Pml*^{+/+} and *Pml*^{−/−} MEF untreated or treated with IFN-γ for 4 h was subjected to microarray analysis. The proportion of genes that are up- or down-regulated (2-fold change) between untreated and IFN-γ-treated cells is shown. (*B*) RNA from immortalized *Pml*^{+/+} and *Pml*^{−/−} MEF treated with IFN-γ for the indicated times was subjected to RPA for IP-10 and GAPDH mRNA levels. Fold induction is shown. Representative of three independent experiments.

treatment up-regulated 217 genes (4.1%) and down-regulated 339 genes (6.3%), whereas in *Pml*^{−/−} MEF, IFN-γ treatment up-regulated 1,056 genes (19.7%) and down-regulated 142 genes (2.7%). Thus, in *Pml*^{−/−} MEF, there is a 5-fold enhancement in IFN-γ up-regulated gene expression. The induction level of affected genes was also different between *Pml*^{+/+} and *Pml*^{−/−} MEF. Representative IFN-γ up-regulated genes are shown, demonstrating higher induction in *Pml*^{−/−} MEF upon IFN-γ treatment compared with *Pml*^{+/+} MEF (Table 1). The enhanced expression of the *IP-10* gene was validated through ribonuclease protection assay (Fig. 2*B*). These data support the hypothesis that PML functions as a negative regulator of IFN-γ-induced gene activation. However, the negative effect of PML on IFN-γ-induced gene expression was observed only in a subset of IFN-γ responsive genes. For *IRF-1*, *SOCS-1*, and *STAT-1*, expression levels were increased in a comparable manner upon IFN-γ treatment in *Pml*^{+/+} and *Pml*^{−/−} MEF (data not

Table 1. Tabulation of IFN-γ up-regulated genes demonstrating higher fold induction in *Pml*^{−/−} MEFs compared with *Pml*^{+/+} MEF

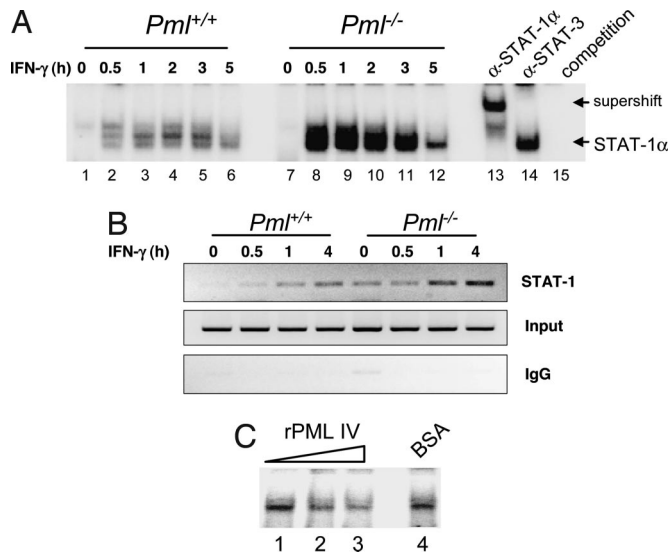| Gene	*Pml*^{−/−} vs. *Pml*^{+/+}
Ifi202B	2.20
Ifi203	2.55
Ifi204	2.75
Ifi205	2.62
Ifi10 (IP-10)	38.85
Clcn3	2.73
Rgs2	5.98
Gnbp3	2.55
TNFaip2	3.68

Choi *et al.*

Fig. 3. PML inhibits DNA binding activity of STAT-1α. (*A*) Nuclear extracts from immortalized *Pml*⁺/⁺ and *Pml*⁻/⁻ MEF treated with IFN-γ for 0–5 h were incubated in the presence of a radiolabeled probe containing a GAS element and subjected to EMSA. Anti-STAT-1α or -STAT-3 antibodies were added to test the specificity of interaction. Binding specificity was also tested by adding a 100-fold molar excess of cold GAS probe (competition). (*B*) Cells were treated with IFN-γ for up to 4 h and fixed by using formaldehyde. Chromatin was sheared and immunoprecipitated by using STAT-1 antibody or normal rabbit IgG, then amplified by RT-PCR using primers designed for the murine CIITA pIV promoter. (*C*) Nuclear extracts from *Pml*⁻/⁻ MEF treated with IFN-γ for 1 h were preincubated with PML IV protein (0–100 ng) for 1 h and then subjected to EMSA (lanes 1–3). BSA was used as a control for the PML protein (lane 4). Representative of three experiments.

Fig. 4. PML interacts with STAT-1 *in vivo*. (*A*) Immortalized *Pml*⁺/⁺ and *Pml*⁻/⁻ MEF were incubated in the absence or presence of IFN-γ for 0.5 and 4 h, and whole-cell lysates were prepared. Cell lysates (1.2 mg) were immunoprecipitated with anti-STAT-1 antibody and subjected to SDS/PAGE for immunoblot analysis with anti-PML antibody. Input samples (5%) were assayed for STAT-1 and PML protein expression by immunoblotting. (*B*) RAW264.7 cells were either untreated or treated with IFN-γ for 0.5 h and processed as described in *A*. (*C*) *Pml*⁻/⁻ MEF transfected with control vector or the PML III expression vector were either untreated or treated with IFN-γ for 0.5 h and immunoprecipitated with anti-STAT-1 antibody. Anti-STAT-1 immunoprecipitates were subjected to immunoblot analysis with anti-PML antibody. Input samples (5%) were also assayed for PML expression by immunoblotting. Representative of three experiments.

shown), suggesting that PML affects a subset of IFN-γ-regulated genes.

PML Inhibits IFN-γ-Induced STAT-1α DNA Binding. The effect of PML on IFN-γ-induced STAT-1α DNA binding was examined. STAT-1α DNA binding was weakly induced by 0.5 h of IFN-γ treatment (lane 2) and diminished by 5 h (lane 6) in *Pml*⁺/⁺ MEF (Fig. 3*A*). In contrast, in *Pml*⁻/⁻ MEF, STAT-1α DNA binding was strongly induced by 0.5 h (lane 8), remained high through 3 h (lanes 9–11), and then diminished by 5 h (lane 12). Anti-STAT-1α antibody supershifted the complex (lane 13), whereas anti-STAT-3 antibody did not (lane 14), confirming the specific interaction between STAT-1α homodimers and the GAS element. Competition with excess unlabeled GAS oligonucleotide abrogated complex formation (lane 15). ChIP was performed to examine STAT-1α binding *in vivo*. STAT-1α recruitment to the CIITA-pIV promoter upon IFN-γ stimulation was more pronounced in *Pml*⁻/⁻ MEF at 1 and 4 h (Fig. 3*B*). These data demonstrate that STAT-1α DNA binding is stronger and prolonged in the absence of PML. We next tested whether PML prevents STAT-1α binding to DNA using an *in vitro* competitive EMSA. Inclusion of recombinant PML partially blocked STAT-1α DNA binding in a dose-dependent manner, using extracts from *Pml*⁻/⁻ cells treated with IFN-γ for 1 h (Fig. 3*C*). These results indicate that PML partially inhibits STAT-1α from binding to DNA, which correlates with increased IFN-γ-induced STAT-1α transcriptional activity in the absence of PML.

IFN-γ Induces PML-STAT-1 Complex Formation. To determine whether PML interacts with STAT-1, *Pml*⁺/⁺ and *Pml*⁻/⁻ MEF were incubated in the absence or presence of IFN-γ for 0.5 or 4 h and then assayed for PML–STAT-1 interaction (Fig. 4*A*). In *Pml*⁺/⁺ MEF, no interaction was detected in unstimulated cells
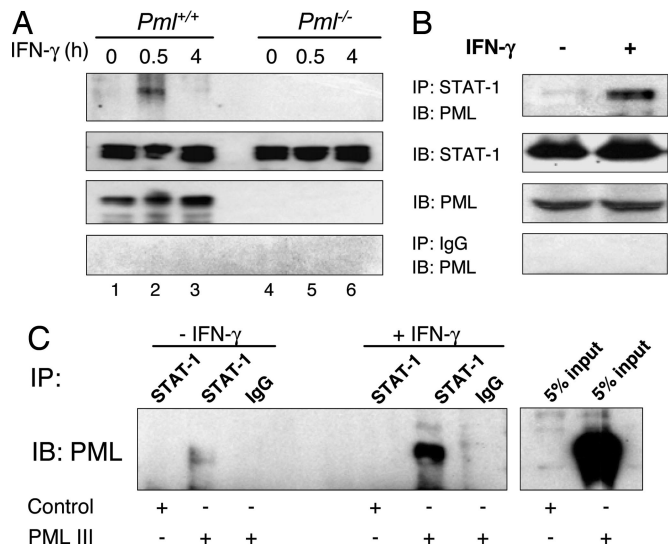
(lane 1); however, IFN-γ induced the association of endogenous PML and STAT-1 at 30 min (lane 2), which diminished by 4 h (lane 3). IFN-γ-induced complex formation was not detectable in *Pml*⁻/⁻ MEF (lanes 4–6). These findings were confirmed in the RAW264.7 macrophage cell line; complex formation occurred between endogenous PML and STAT-1 upon IFN-γ treatment (Fig. 4*B*). We next determined whether reconstitution of PML in *Pml*⁻/⁻ MEF could result in complex formation with STAT-1α. Weak PML–STAT-1 complex formation was detected in untreated *Pml*⁻/⁻ MEF restored with PML; however, enhanced complex formation was detected in IFN-γ-treated *Pml*⁻/⁻ MEF restored with PML (Fig. 4*C*). These results indicate that IFN-γ treatment results in PML–STAT-1 complex formation. To determine which domain(s) of PML is important for the PML–STAT-1 interaction, we used *in vitro*-translated PML mutants (26) and incubated them with immobilized STAT-1 using anti-STAT-1 antibody or control IgG [supporting information (SI) Fig. 7*A*]. PML mutants lacking the C terminus were not able to bind to STAT-1 (SI Fig. 7*B*, lanes 2 and 3), whereas binding to STAT-1 was observed with full length PML and two PML mutants with N terminus deletions (SI Fig. 7*B*, lanes 1, 4, and 5). These results indicate that the C terminus of PML is important for STAT-1 binding.

IFN-γ Enhances PML-STAT-1 Colocalization in the Nucleus. To analyze PML-STAT-1 colocalization, *Pml*⁺/⁺ MEF were incubated in the absence or presence of IFN-γ for 0.5 h, fixed, and then stained for total STAT-1 (Fig. 5*A*, green) followed by staining for PML (red). STAT-1 was mainly localized in the cytoplasm in the absence of IFN-γ, and nuclear translocation occurred upon IFN-γ treatment (Fig. 5*A*). PML was detectable in the nuclear compartment in unstimulated cells, and intensity of staining was enhanced after IFN-γ treatment (Fig. 5*A*). PML-STAT-1 colo-
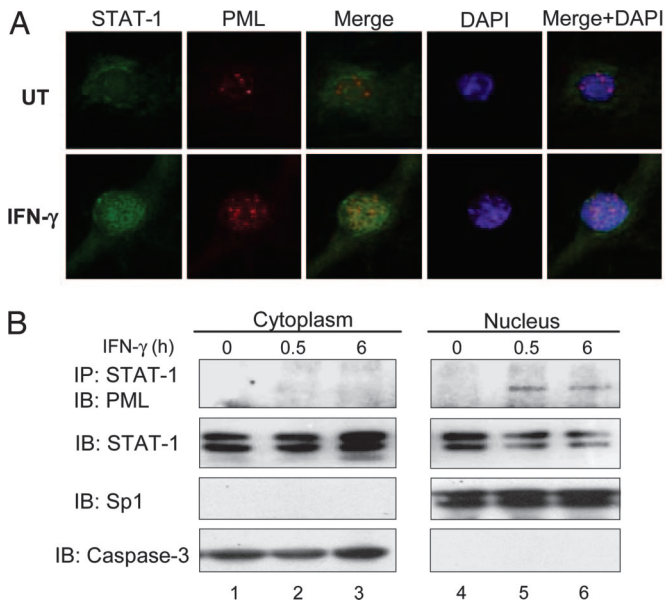
Choi *et al*.

Fig. 5. PML and STAT-1 colocalize upon IFN-γ treatment. (*A*) Immortalized *Pml*^{+/+} MEF were incubated with IFN-γ for 0.5 h, stained with rabbit polyclonal anti-STAT-1 (green) and mouse monoclonal anti-PML (red) antibodies, and analyzed by immunofluorescent microscopy. Representative of three experiments. (*B*) Immortalized *Pml*^{+/+} MEF were incubated in the absence or presence of IFN-γ for 0.5 and 6 h. Cytoplasmic and nuclear fractions were prepared and assayed for PML–STAT-1 complex formation by coimmunoprecipitation. Input samples from the cytoplasmic and nuclear fractions were subjected to immunoblotting to detect caspase-3 and Sp1, respectively. Representative of three experiments.

calization was rarely detected in the absence of IFN-γ, whereas IFN-γ treatment enhanced PML-STAT-1 colocalization in the nucleus (Fig. 5*A*). Similar results were observed for tyrosine phosphorylated STAT-1 and PML colocalization (data not shown). Staining with isotype control antibodies was performed to verify specificity (data not shown). We further assessed the cellular localization of the PML-STAT-1 complex using cytoplasmic and nuclear fractions. In *Pml*^{+/+} MEF, the IFN-γ-induced PML-STAT-1 complex was detected only in the nuclear fraction at 0.5 h, with decreased complex formation observed at 6 h (Fig. 5*B*). These results indicate that IFN-γ induces STAT-1 nuclear localization and PML-STAT-1α complex formation in the nucleus.

PML Does Not Influence STAT-1α Phosphorylation. Cytoplasmic isoforms of PML have recently been described that affect signal transduction pathways, thus it is possible that PML may influence STAT-1α phosphorylation within the cytoplasm. *Pml*^{+/+} and *Pml*^{−/−} MEF were incubated with IFN-γ for 0–6 h, then STAT-1α tyrosine and serine phosphorylation was examined (SI Fig. 8). IFN-γ-induced STAT-1α phosphorylation on both tyrosine 701 and serine 727 was comparable in both cells, indicating that PML does not affect STAT-1α phosphorylation.

Discussion

We have provided evidence for a function of PML as a negative regulator of the IFN-γ signaling pathway. Using *Pml*^{+/+} and *Pml*^{−/−} MEF, we demonstrated that the absence of PML enhanced IFN-γ-induced STAT-1α transcriptional activity and led to an enhancement in the number of endogenous IFN-γ-upregulated genes and in their level of induction. The presence of PML inhibited IFN-γ-induced STAT-1α DNA-binding activity as well. These results strongly suggest a role for PML as a
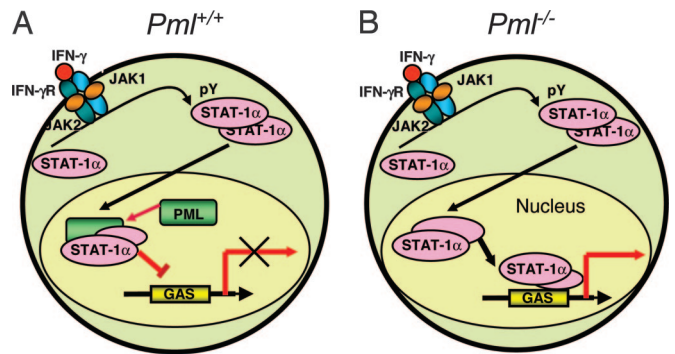

Fig. 6. Proposed model for the role of PML in regulating IFN-γ signaling. (*A*) IFN-γ-induced STAT-1α DNA-binding and transcriptional activities are reduced in the presence of PML. Because IFN-γ induces the colocalization and formation of a PML-STAT-1α complex in the nucleus, we propose that PML may inhibit the binding of STAT-1α to DNA and thus control its activity, leading to a dampening of IFN-γ inducible genes. (*B*) In the absence of PML, STAT-1α binds to GAS elements, perhaps with higher affinity, and IFN-γ inducible gene expression is heightened.

negative regulator in the IFN-γ signaling cascade, resulting in reduced STAT-1α transcriptional activity.

Because IFN-γ induced the colocalization and formation of a PML–STAT-1α complex in the nucleus, we propose that PML may inhibit the binding of STAT-1α to DNA through protein–protein interactions and thus control STAT-1α transcriptional activity (Fig. 6). It is possible that the STAT–1α-PML complex is less favorable to bind DNA compared with STAT-1α itself or less efficient in recruiting other transcription factors and/or coactivators necessary for optimal IFN-γ-mediated transcription. Considering that PML partially inhibits the binding of STAT-1α to DNA, this suggests that nuclear STAT-1α cannot bind effectively to DNA in the presence of PML (Fig. 6*A*). In this study, we demonstrated that PML inhibited binding of STAT-1α homodimers to GAS elements in response to IFN-γ, whereas Kawasaki *et al.* (27) determined that PML inhibited STAT-3 DNA binding in response to G-CSF stimulation. In this regard, PML was shown to suppress IL-6-induced STAT-3 activity (27), whereas we have observed aberrant STAT-3 activation in the absence of PML (Y.-H.C. and E.N.B., unpublished observations). These findings and the results herein indicate the PML influences both the STAT-1α and -3 signaling pathways, and that PML may be a more general regulator of the STAT family of proteins.

The PML protein interacts with numerous proteins (18–24); however, the domain(s) of PML required for interaction varies. As examples, p53 binds to the C-terminal portion of PML (24), whereas Nur77 requires the coiled-coil domain of PML for interaction (21). The STAT-3 protein binds PML through the B-box zinc finger and C-terminal domains (27). Our results indicate that the C terminus of PML is important for STAT-1 binding. We also determined that PML mutants lacking the C-terminal domains, which do not bind STAT-1α, also do not inhibit STAT-1α transcriptional activity in *Pml*^{−/−} MEF (data not shown). These data demonstrate that PML interacts with STAT-1α by its C terminus, and that this complex formation inhibits the transcriptional activity of STAT-1α.

PIAS1 is a nuclear protein involved in the negative regulation of STAT-1α transcriptional activity by inhibiting DNA binding of STAT-1α (7). PIAS1 deficiency promotes enhanced recruitment of STAT-1 to the promoter of STAT-1-dependent genes; however, this effect occurs in a gene-specific manner. The specificity of PIAS1 is due to the DNA-binding affinity of STAT-1-binding sites present in the promoters of target genes, with PIAS1 inhibiting the DNA-binding activity of STAT-1 more

efficiently on a weak than on a strong binding site (7). Although STAT-1α DNA binding is negatively affected by PML, microarray data demonstrated that only a subset of IFN-γ responsive genes were affected by PML, similar to results reported from PIAS1-deficient mice (7). Interestingly, IFN-γ induction of *IP-10* and *Ifi203* was higher in both PIAS1- and PML-deficient cells, whereas IFN-γ-induced *Irf1* and *Socs1* gene expression was not affected by either PIAS1 or PML deficiency (7). The results from our study suggest that PML functions in the IFN-γ signaling pathway as a negative regulator, tuning and controlling the extent and duration of signaling, rather than as a global inhibitor. The expression level of PIAS1 in *Pml*$^{+/+}$ and *Pml*$^{-/-}$ MEF in the absence or presence of IFN-γ was comparable, indicating that PIAS1 was not affected by the absence of PML (data not shown). There are other negative regulators of the IFN-γ-mediated JAK-STAT pathway. The TRADD protein functions by forming a complex with STAT-1α within the nucleus and inhibiting STAT-1α transcriptional activity (8). Activated vitamin D hormone suppresses numerous IFN-γ-inducible genes in macrophages (9). This inhibitory mechanism is independent of STAT-1α; rather, it depends on the expression and localization of the vitamin D receptor (9). Annexin V was shown to associate with the IFN-γ receptor upon IFN-γ treatment and to inhibit activation of JAK2 and STAT-1α (28). These data indicate that IFN-γ activation of the JAK-STAT pathway can be negatively regulated at many levels and in different cellular compartments.

PML is essential for induction of apoptosis by diverse stimuli. PML promotes apoptosis by a TNF-mediated pathway and sensitizes cells to apoptosis by inhibiting the NF-κB survival pathway. This is accomplished by PML binding to p65 and interfering with its binding to NF-κB target genes (29). Another pathway implicated in apoptotic responses is the p38 MAPK pathway, which is also negatively regulated by PML (30). The effect of PML on signal transduction is complex, having both positive (TGF-β pathway) and inhibitory effects (STAT, NF-κB, and p38 MAPK pathways). We have provided evidence that PML negatively regulates the IFN-γ signaling pathway and selectively inhibits expression of a subset of IFN-γ-inducible genes. The inhibitory effect of PML occurs by inhibiting STAT-1α DNA binding and transcriptional activation (Fig. 6). It will be interesting to compare the inhibitory effects of both PIAS1 and PML on STAT-1α DNA binding and to determine whether these two nuclear proteins function in a coordinated fashion to inhibit expression of a subset of IFN-γ-inducible genes.

Materials and Methods

Cells. Primary and immortalized *Pml*$^{+/+}$ and *Pml*$^{-/-}$ MEF were established and maintained as described (26). The murine macrophage cell line RAW264.7 was maintained as described (8).

Reagents and Antibodies. Recombinant murine IFN-γ was purchased from R&D Systems (Boston, MA). Antibodies to PML (mouse monoclonal), STAT-1, and *p*-S727-STAT-1 were purchased from Upstate Biotechnology (Lake Placid, NY). Antibody to *p*-Y701-STAT-1 was purchased from Cell Signaling Technology (Beverly, MA). Rabbit polyclonal antibody to PML was purchased from Santa Cruz Biotechnology (Santa Cruz, CA), and antiactin antibody was purchased from Sigma (St. Louis, MO).

Plasmids, Transient Transfection, and Reporter Assays. For reconstitution of PML in *Pml*$^{-/-}$ MEF, pCMV-Tag2B-PML-I, pSG5-PML-III, and pCMV-Tag2B-PML-IV expression vectors were used (26). The pET-33b-PML-IV vector was used for purification of recombinant PML protein (26). The GAS4-luc construct, minimal CIITA promoter construct (CIITAp-D4) and full-length CIITA promoter construct (CIITA) have been described

(8, 31). Transient transfections were performed with FuGENE 6, Roche Diagnostics (Indianapolis, IN). For reporter assays, 0.4 μg of the GAS-containing constructs was transiently transfected into 2×10^5 *Pml*$^{+/+}$ or *Pml*$^{-/-}$ MEF, with 0.1 μg of the pCMV-β-galactosidase vector to normalize for transfection efficiency. Increasing concentrations (0–2.0 μg) of the PML expression vectors were cotransfected with those constructs in some experiments. Cells recovered for 12 h before treatment with IFN-γ (10 ng/ml) for 16 h, then luciferase activity was measured (8). The luciferase activity of each sample was normalized to β-galactosidase activity to yield relative luciferase activity (RLA). Fold induction was calculated as the ratio of RLA between IFN-γ and untreated samples. The data were analyzed by Student's t test, and a value of $P < 0.05$ was considered statistically significant.

RNA Isolation, Microarray, and Ribonuclease Protection Assay (RPA). Total cellular RNA was isolated from cells by using TRIzol (Invitrogen Life Technologies, Carlsbad, CA). Five micrograms of RNA was subjected to microarray analysis by using the Mouse Genome 430 2.0 GeneChip (Affymetrix) and subsequent data analysis using the Microarray Suite and the Data Mining Tools (Affymetrix) was performed by the University of Alabama at Birmingham Comprehensive Cancer Center Gene Expression Shared Facility. The experimental procedure was conducted by following the standard Affymetrix protocol. RNA quality and quantity were confirmed with the Agilent Bioanalyzer 2100 system (Agilent Technologies, Palo Alto, CA). The mCK-5 multiriboprobe was purchased from PharMingen (San Diego, CA), and 15 μg of total RNA was hybridized with the riboprobes, as described (8). Quantification of the protected RNA fragments was performed with the PhosphorImager (Molecular Dynamics, Sunnyvale, CA). Values for IP-10 mRNA expression were normalized to GAPDH mRNA levels.

Nuclear Extracts and EMSA. EMSA was performed with 10 μg of nuclear extracts, as described (8). Nuclear extracts from *Pml*$^{+/+}$ and *Pml*$^{-/-}$ MEF treated with IFN-γ for 0–5 h were incubated with a GAS oligonucleotide end-labeled with [^{32}P]ATP for 30 min. For competition and supershift experiments, a 100 molar excess of cold oligonucleotide or 1 μg of anti-STAT-1α or -3 antibodies was added to the nuclear extracts for 30 min before the addition of labeled probe. For *in vitro* competitive EMSA experiments, nuclear extracts from *Pml*$^{-/-}$ MEF treated with IFN-γ for 1 h were preincubated with recombinant PML protein (0–100 ng) for 1 h and then incubated with the [^{32}P] end-labeled GAS oligonucleotide for 30 min. BSA (100 ng) was used as a control for the PML protein. Bound and free DNA were resolved by electrophoresis through a 6% polyacrylamide gel and exposed for autoradiography.

ChIP Assay. ChIP analysis was performed as described (8). After IFN-γ stimulation (0–4 h), cells were fixed with 1% formaldehyde for 15 min and washed with cold PBS. Nuclei were isolated as described (8), and chromatin was sheared by sonication. Sheared chromatin solution was precleared with salmon sperm DNA-saturated protein A/G Sepharose beads and then precipitated with 4 μg of anti-STAT-1 or isotype-matched control IgG overnight at 4°C. Immune complexes were incubated with salmon sperm DNA-saturated protein A/G Sepharose beads for 3 h at 4°C and were washed extensively. To reverse crosslinks, samples were incubated at 65°C overnight. After proteinase K digestion, DNA was recovered by using the Qiagen miniprep kit (Valencia, CA). Purified DNA was analyzed by PCR by using a primer pair designed for the murine CIITA-pIV promoter containing a functional GAS element: 5′-GAGGGGTCCTCT-GGAAAGAC-3′ and 5′-GCAGTCTCCTGGCAGCTATC-3′.

Coimmunoprecipitation and Immunoblotting. $Pml^{+/+}$ and $Pml^{-/-}$ MEF were incubated with medium or IFN-γ (10 ng/ml) for various time points, and coimmunoprecipitation was performed as described (8). Cleared lysates were incubated overnight with 3 μg of rabbit anti-STAT-1 and an additional incubation for 3 h with 50 μl of protein A/G bead slurry at 4°C. After washing, the samples were separated on 8% SDS/PAGE and analyzed by immunoblotting with monoclonal or polyclonal anti-PML antibodies (1 μg/ml) for detection of endogenous PML–STAT-1 interaction. Coimmunoprecipitation of cytoplasmic and nuclear proteins was performed as described (8). Two milligrams of nuclear and cytoplasmic extracts was subjected to immunoprecipitation with anti-STAT-1 antibody and immunoblotting with anti-PML. Anti-Sp1 and -caspase-3 antibodies were used to demonstrate separation of the nuclear and cytoplasmic fractions, respectively. For immunoblotting, whole cell lysates were subjected to SDS/PAGE, and blots were probed with Y701-phospho-STAT-1, S727-phospho-STAT-1, total STAT-1, PML, or actin antibodies.

His-Fusion PML Protein Expression, *in Vitro* Translation, and Binding Assay. The pET-33b plasmid encoding PML IV was used as a source of His-fusion PML protein (26). For His-PML protein expression, the BL21 competent *Escherichia coli* strain (Novagen, Madison, MD) and isopropyl-1-thio-β-D-galactopyranoside (IPTG) were used. After 4 h of induction with 0.1 mM IPTG, the bacteria were collected, lysed, incubated with 1 μg of lysozyme for 30 min on ice, and then disrupted by sonication. Purification of the His-PML protein was performed by using a Ni-NTA spin column purchased from Qiagen. The protein concentration of the His-fusion PML protein was determined, and purity was assessed by Coomassie brilliant blue staining. For *in vitro* translation, PML full length and mutant proteins (26) were expressed under the T3 promoter by using the TNT-coupled transcription/translation system with [^{35}S]methionine (Promega, Madison, WI). For binding assays, whole-cell lysates containing endogenous STAT-1 protein were precleared and incubated with anti-STAT-1 antibody or rabbit IgG overnight at 4°C, then immunoprecipitated with protein A/G beads for an additional 3 h. STAT-1-protein A/G beads or rabbit IgG protein A/G beads were washed extensively and incubated with ^{35}S-labeled PML proteins in binding buffer overnight at 4°C. Beads were washed five times with binding buffer, then bound proteins were analyzed by SDS/PAGE.

Immunofluorescence Assay (IFA). IFA was performed as described (8). $Pml^{+/+}$ MEF were incubated in the absence or presence of IFN-γ (10 ng/ml) for 30 min. Cells were stained with anti-STAT-1 for 1 h, rinsed three times with PBS, and then stained with goat anti-rabbit Alexa^{488} (Molecular Probes, Eugene, OR) for 45 min. Cells were rinsed again with PBS, followed by staining with mouse anti-PML antibody for 1 h. Cells were then rinsed three times in PBS and stained with goat anti-mouse Alexa^{594} for 45 min. Cells were then stained with DAPI. Images were obtained with an Olympus (Melville, NY) IX70 digital camera and analyzed with IPLab 3.2 software (Scanalytics, Inc., Fairfax, VA).

1. Regis G, Conti L, Boselli D, Novelli F (2006) *Trends Immunol* 27:96–101.
2. Ramana CV, Gil MP, Schreiber RD, Stark GR (2002) *Trends Immunol* 23:96–101.
3. Decker T, Kovarik P (2000) *Oncogene* 19:2628–2637.
4. Shuai K, Liu B (2003) *Nat Rev Immunol* 3:900–911.
5. Yasukawa H, Misawa H, Sakamoto H, Masuhara M, Sasaki A, Wakioka T, Ohtsuka S, Imaizumi T, Matsuda T, Ihle JN, Yoshimura A (1999) *EMBO J* 18:1309–1320.
6. Qu CK (2002) *Biochim Biophys Acta* 1592:297–301.
7. Liu B, Mink S, Wong KA, Stein N, Getman C, Dempsey PW, Wu H, Shuai K (2004) *Nat Immunol* 5:891–898.
8. Wesemann DR, Qin H, Kokorina N, Benveniste EN (2004) *Nat Immunol* 5:199–207.
9. Helming L, Bose J, Ehrchen J, Schiebe S, Frahm T, Geffers R, Probst-Kepper M, Balling R, Lengeling A (2005) *Blood* 106:4351–4358.
10. Borrow J, Goddard AD, Sheer D, Solomon E (1990) *Science* 249:1577–1580.
11. de The H, Lavau C, Marchio A, Chomienne C, Degos L, Dejean A (1991) *Cell* 66:675–684.
12. Goddard AD, Borrow J, Freemont PS, Solomon E (1991) *Science* 254:1371–1374.
13. Kakizuka A, Miller WH, Jr, Umesono K, Warrell RP, Jr., Frankel SR, Murty VV, Dmitrovsky E, Evans RM (1991) *Cell* 66:663–674.
14. Pandolfi PP, Grignani F, Alcalay M, Mencarelli A, Biondi A, LoCoco F, Grignani F, Pelicci PG (1991) *Oncogene* 6:1285–1292.
15. Regad T, Chelbi-Alix MK (2001) *Oncogene* 20:7274–7286.
16. Jensen K, Shiels C, Freemont PS (2001) *Oncogene* 20:7223–7233.
17. Ching RW, Dellaire G, Eskiw CH, Bazett-Jones DP (2005) *J Cell Sci* 118:847–854.
18. LaMorte VJ, Dyck JA, Ochs RL, Evans RM (1998) *Proc Natl Acad Sci USA* 95:4991–4996.
19. Wu WS, Vallian S, Seto E, Yang WM, Edmondson D, Roth S, Chang KS (2001) *Mol Cell Biol* 21:2259–2268.
20. Khan MM, Nomura T, Kim H, Kaul SC, Wadhwa R, Shinagawa T, Ichikawa-Iwata E, Zhong S, Pandolfi PP, Ishii S (2001) *Mol Cell* 7:1233–1243.
21. Wu WS, Xu ZX, Ran R, Meng F, Chang KS (2002) *Oncogene* 21:3925–3933.
22. Vallian S, Gaken JA, Gingold EB, Kouzarides T, Chang KS, Farzaneh F (1998) *Oncogene* 16:2843–2853.
23. Cairo S, De Falco F, Pizzo M, Salomoni P, Pandolfi PP, Meroni G (2005) *Oncogene* 24:2195–2203.
24. Guo A, Salomoni P, Luo J, Shih A, Zhong S, Gu W, Pandolfi PP (2000) *Nat Cell Biol* 2:730–736.
25. Lin HK, Bergmann S, Pandolfi PP (2004) *Nature* 431:205–211.
26. Bernardi R, Scaglioni PP, Bergmann S, Horn HF, Vousden KH, Pandolfi PP (2004) *Nat Cell Biol* 6:665–672.
27. Kawasaki A, Matsumura I, Kataoka Y, Takigawa E, Nakajima K, Kanakura Y (2003) *Blood* 101:3668–3673.
28. Leon C, Nandan D, Lopez M, Moeenrezakhanlou A, Reiner NE (2006) *J Immunol* 176:5934–5942.
29. Wu WS, Xu ZX, Hittelman WN, Salomoni P, Pandolfi PP, Chang KS (2003) *J Biol Chem* 278:12294–12304.
30. Shin J, Park B, Cho S, Lee S, Kim Y, Lee SO, Cho K, Lee S, Jin BS, Ahn JH, Choi EJ, Ahn K (2004) *J Biol Chem* 279:40994–41003.
31. Dong Y, Tang L, Letterio JJ, Benveniste EN (2001) *J Immunol* 167:311–319.